CONSIGLIO NAZIONALE DELLE RICERCHE
Istituto di Fisica Atomica e Molecolare

CNR - Area della Ricerca di Pisa
Loc. S. Cataldo, Ghezzano
56010 Pisa, Italy

Rapporto Scientifico Interno N.3/2000 del 21-11-2000

SPACE RESOLVED X-RAY SPECTROSCOPY OF LASER-PRODUCED PLASMAS

Leonida A. GIZZI, Luca LABATE, Marco GALIMBERTI, Azenio SALVETTI
IFAM-CNR

Abstract:

We have developed a micrometer-resolution space resolving X-ray spectrometer aimed at the investigation of laser-produced plasmas. The spectrometer was based upon a TlAP crystal set in a first-order Bragg configuration and used a cooled CCD camera as a detector and a 10 m width slit between the target-plasma and the crystal as a space-resolving device. This configuration enabled us to obtain high dynamic range X-ray spectra of an aluminium plasma in the range from 5.5 to 8 with a spatial resolution of about 20 m inside the X-ray emitting region. These measurements allowed us to obtain a spatial profile of electron temperature which was found to vary from 180 eV in the overdense region up to about 650 eV in the underdense coronal region

SPACE RESOLVED X-RAY SPECTROSCOPY OF LASER-PRODUCED PLASMAS

Leonida A. GIZZI, Luca LABATE, Marco GALIMBERTI, Azenio SALVETTI

Intense Laser Irradiation Laboratory - IFAM
Area della Ricerca del CNR, Ghezzano, 56010 - Pisa, Italy

Abstract: *We have developed a micrometer-resolution space resolving X-ray spectrometer aimed at the investigation of laser-produced plasmas. The spectrometer was based upon a TlAP crystal set in a first-order Bragg configuration and used a cooled CCD camera as a detector and a 10 m width slit between the target-plasma and the crystal as a space-resolving device. This configuration enabled us to obtain high dynamic range X-ray spectra of an aluminium plasma in the range from 5.5 to 8 with a spatial resolution of about 20 m inside the X-ray emitting region. These measurements allowed us to obtain a spatial profile of electron temperature which was found to vary from 180 eV in the overdense region up to about 650 eV in the underdense coronal region.*

1. INTRODUCTION

X-ray spectroscopy of self-emission from hot plasmas is extensively used to measure plasma properties in a variety of physical conditions, from the low-density tokamak-type plasmas to the higher density laser-plasmas[1]. In the case of laser-plasmas, besides the obvious case of the coronal region, X-ray based diagnostics are particularly useful in the study of the overdense region which is otherwise inaccessible to optical diagnostic methods [2,3].
In its simplest form X-ray spectroscopy provides X-ray spectra integrated over the entire extent of the X-ray emitting source. This is well suited when the plasma under investigation is relatively small and substantially homogeneous as, for example, in the case of discharges in gases, laser interactions with preformed plasmas or gas-jets.
In the general case of laser interaction with solid matter a strongly inhomogeneous plasma is generated in terms of electron temperature or density. In this case space integration only provides a somewhat averaged information which often masks important information of the status of the plasma.
Space-resolved measurements are therefore necessary to properly characterise these plasmas and in particular plasmas produced by laser irradiation of solid materials. On the other hand, this technique can also be profitably used to study localised laser-heating phenomena such as filamentation or self-focusing, strongly correlated plasmas of high density[4] or the gain region for X-ray lasers [5].
Finally, the knowledge of spatial characteristics of laser produced plasmas allows X-ray sources for applications to be optimised (see [6] and references therein).
The main obstacle to an extensive use of this technique is that in order to obtain the required micron-scale resolution, a very narrow slit must be used, with a consequent dramatic reduction of the X-ray flux. For this reason this class of experiments in the past has been limited to relatively low resolution (large slits) and low spectral dispersion.
The recent availability of high dynamic range CCD X-ray detectors makes now possible to perform these studies on an unprecedented spatial/spectral resolution, with the possibility of reaching the micron resolution level (X-ray spectro-microscopy).
In this report we describe our experimental technique to obtain space resolved spectra of laser-produced plasmas and we show that the combination of a back-illuminated CCD detectors and a high diffraction efficiency crystal result in high sensitivity instrument well suited for high spatial/spectral resolution studies of small(10-1000 micrometer) X-ray sources.

2. EXPERIMENTAL SETUP

The experimental setup inside the interaction chamber is shown in Fig1. The object plasma is produced by focusing with an *f/4* optics a Nd:YLF laser beam (λ= 1.053 μm) onto an Al cylindrical target. The angle of incidence was set to be 20 degrees to avoid detrimental back-reflections from the plasma. The laser, transversally and longitudinally monomode, provided an energy up to 3J in each 3ns (FWHM) gaussian pulse. Shot to shot fluctuations in the total energy delivered on the target were limited to a 10 %. Data obtained with larger variations have not been taken into account. The laser beam had a gaussian spatial distribution with a waist of about 6 μm (FWHM) and a Rayleigh length of about 100 μm, resulting in an intensity on the target up to $5 \times 10^{14} W/cm^2$. A flat *thallium hydrogen phthalate* (TlAP) crystal (2d = 25.9), set in a first-order

Bragg configuration, was coupled to a back-illuminated Peltier cooled CCD camera to spectrally resolve X-ray emission from the plasma. The spectrometer was ser to investigate a spectral region from approximately 5.5 to 8 which includes the K-shell spectral lines from H-like and He-like aluminium. The spectrometer was placed at an angle of 45 degrees with respect to the laser beam axis (see Fig.1).

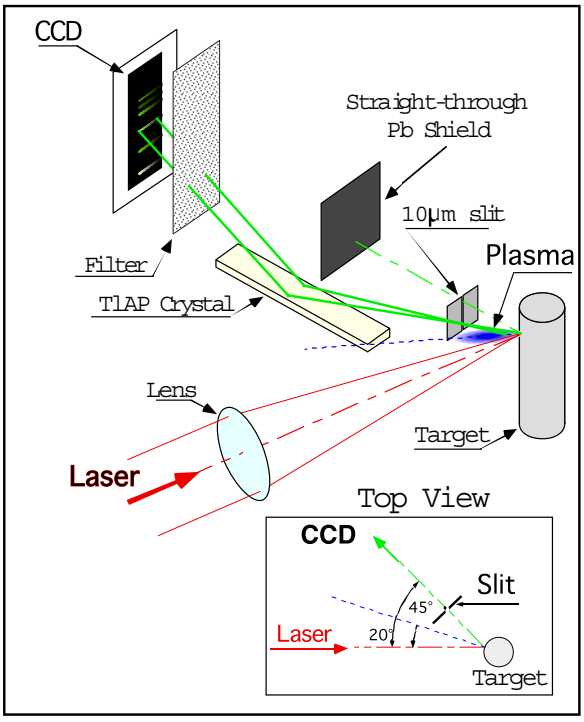

***Fig.1**. Schematic set-up of the experiment showing the arrangement of the crystal spectrometer and the geometry of the interaction.*

Spectral resolution is determined by the size of the emitting region, by the size of the CCD pixels and by the specific properties of the crystal (rocking curve). Taking into account all these effects, the resolving power of our instrument can be approximately given by [7]

$$\frac{\lambda}{\delta\lambda} = \sqrt{\frac{\tan^2\vartheta_B}{(\delta\vartheta_c)^2 + (\delta x/L)^2 + (\delta y/L)^2}} \qquad (1)$$

where ϑ_B is the Bragg angle, $\delta\vartheta_c \approx 10^{-4}$ rad is the TlAP rocking angle, $L \approx 20$ cm is the total distance between the source to the CCD, $\delta x \approx 100\,\mu$m and $\delta y \approx 24\,\mu$m are respectively the size of the emitting region and of the CCD pixel. Thus for $\lambda = 7\,\mu$m we obtain a resolving power $\lambda/\delta\lambda \approx 2\times10^{-3}$. The direction perpendicular to the spectral axis in the plane of the CCD array provides the required spatial information on the spectrum. In order to accomplish this task a 10 μm width slit was used (see Fig.1), which allowed a spatial resolution of about 20 μm in the object plane, along the direction perpendicular to the target surface.

3. RESULTS AND DISCUSSION

3.1 SPATIALLY INTEGRATED SPECTRA

It is interesting to compare a space-integrated spectrum with a space-resolved spectrum obtained using the set-up of Fig.1. Fig.2 shows a space-integrated spectrum in the range from 5.5 to 8 obtained using the same set-up but without the use of a slit. The resonance lines from Al XI (lithium-like), Al XII (helium-like) and Al XIII (hydrogen-like) ions are clearly visible, together with their satellites.
Also visible is the intercombination line (IC), which results from the $1s2p\,^3P \rightarrow 1s^2\,S$ transition in Al XII. This transition, normally forbidden by the spin selection rule in *L-S* coupling, becomes allowed due to the mixing of the $1s2p\,^3P$ and $1s2p\,^1P$ states in helium-like ions.

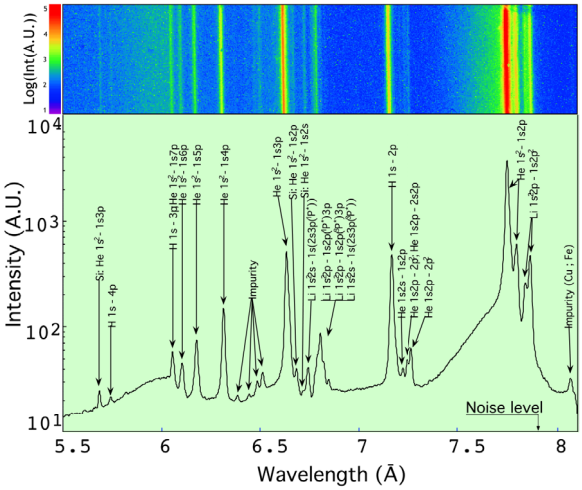

***Fig.2**. Spatially integrated spectrum of X-ray radiation in the range from 5.5 to 8 emitted by an Al.plasma generated from laser interaction with a solid target.*

A comparison of the measured line ratios with the predictions of the steady state atomic physics code RATION [8] can yield a value of the electron temperature averaged over the entire plasma emitting

region. The code was set to calculate atomic populations and line intensities assuming a collisional-radiative equilibrium (CRE) for a steady-state, homogeneous plasma of a given size, temperature and density, including opacity effects. A discussion about the applicability of this code to our experimental conditions is given in reference [9].
It is clear however that additional information is needed to the code including plasma dimension along the line of sight (to take into account the opacity effects) and the averaged density of the emitting region.

3.1.1 Source dimensions and opacity effects

The size of the emitting region for each spectral line in the direction of spectral dispersion can be determined by the line-width, provided Doppler and pressure broadening are much smaller than instrumental broadening. In the configuration of our spectrometer an element of size δx of the source induces a broadening $\delta\lambda_o$ of the observed line at wavelength λ given by:

$$\delta\lambda_o = \sqrt{\delta\lambda_c{}^2 + \left(\frac{\delta x}{L\tan\vartheta_B}\right)^2 \lambda^2} \qquad (2)$$

where ϑ_B and L are as in formula (1) and $\delta\lambda_c = \delta\vartheta_c\,\lambda_B / \tan\vartheta_B$ is the broadening due to the crystal rocking curve. Of course, given the line-width $\delta\lambda_o$, the crystal properties and the geometry of the spectrometer, Eq.(2) can also be used to estimate the source size δx.
We note here that in some circumstances the geometrical parameter L in general is known only approximately due to practical difficulties. However this parameter can be retrieved with great precision by studying the pattern of the spectral lines in the plane of the CCD matrix. In fact, a given wavelength λ emitted by a point source and dispersed by the crystal is collected in a curved path resulting from the intersection of the CCD matrix plane with a cone having the vertex in the virtual source position. Position and curvature of these paths depend on the geometrical parameters of the spectrometer, including L. The finite extent of the source does not affect this consideration, resulting only in a broadening of the lines. The value of L estimated using this procedure was found to be more accurate that the value obtained fform a direct measurement.
The size of the emitting region was determined for three different spectral lines, namely Heα, Heβ and Lyα.. Geometrical considerations, together with the assumption of cylindrical symmetry around the main plasma expansion direction, allowed us to get the transverse size of the emitting regions, i.e. the size along a direction perpendicular to the symmetry axis,. The values obtained from this analysis are $\delta x = 78 \pm 7\,\mu\text{m}$, $\delta x = 66 \pm 5\,\mu\text{m}$ and $\delta x = 54 \pm 4\,\mu\text{m}$ respectively for the Heα, Heβ and Lyα lines. These values do not depend (within 10% variations) upon the position of the target on the laser beam propagation axis in an interval of about 10 Rayleigh lengths around the beam waist. The size of the emission region of the hydrogen-like Lyα line is smaller than the corresponding size of helium-like lines. This is reasonable if we consider that these sizes are significantly greater than the size of the laser focal spot and that the electron temperature in the transverse direction drops due to the plasma expansion. It is important to point out that these values refer to the source transverse dimensions integrated over the whole plasma extent. However, by comparing different spectral line intensity ratios with the predictions of the code RATION we were able to attribute to the source an electron density between 5×10^{20} and 10^{21} el/cm^{-3}. This result is consistent with previous studies [10] which showed that most of the X-ray radiation comes from a plasma region which has a sufficiently high density and where substantial absorption of laser energy takes place.
In the case of a plasma generated by irradiation of a solid target by a Nd laser light this region is located at densities below 10^{21} el/cm^{-3} which is also the critical density for the Nd laser wavelength. We also observe that this result is in agreement with density measurements in similar conditions obtained in a previous work [11]. Thus the values of source sizes given above should be considered as plasma transverse dimensions in front of the target for densities equal or lower than the critical density.
Finally, we took into account plasma opacity by considering the effects on temperature measurements from the spatially integrated spectra over a plasma size ranging from 50 to 100 m.

3.1.2 Spatially integrated electron temperature

Spectra like the one shown in Fig.2 were obtained for several positions of the target plane with respect to the laser beam waist plane. The result of these measurements is summarised in the plot of Fig.3 which shows the observed Lyα to Heα intensity ratio for different positions of the target along the laser beam propagation axis. We can now compare this plot with the same intensity ratio (Fig.4) as calculated by the code RATION for a range of temperatures and densities and assuming a plasma size of 75 m. According to this plot, the ratio is an increasing function of the temperature.

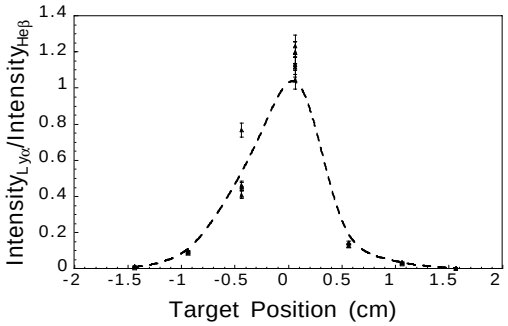

Fig.3 *Measured Lyα to Heα intensity ratio as a function of the target position along the laser propagation axis with respect to the beam waist.*

Therefore, according to Fig.3, a maximum of the electron temperature takes place near the beam waist. As discussed above, it is reasonable to consider a range of electron densities from 5×10^{20} and 10^{21} el/cm^3 for the region of the plasma from which this X-ray radiation takes place.Fig.5 shows the retrieved electron temperature as a function of the target position corresponding to these density values. In each plots the uncertainties are mainly determined by the choice of the opacity level (i.e. of the source size) rather than by the actual experimental errors.

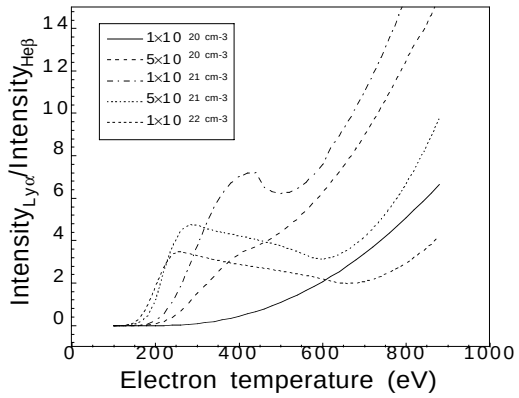

Fig.4 *Calculated Lyα to Heα intensity ratio as a function of the electron temperature and for five different electron densities.*

According to these plots, when the beam waist is on the target plane, the plasma electron temperature ranges between about 240 eV for $n_e = 10^{21}$el/cm^3 and 280 eV for $n_e = 5\times10^{20}$el/cm^3. Temperature falls down to about 140 eV when the target is 1.5 mm away from the waist position.

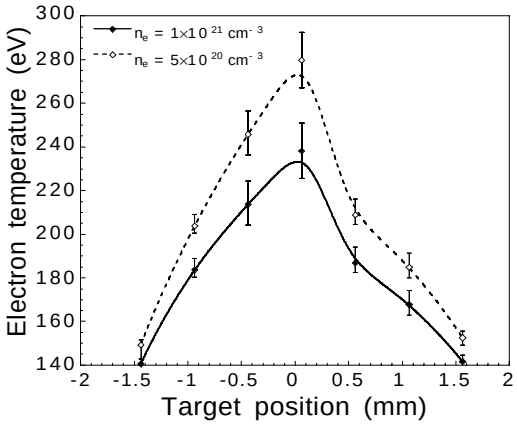

Fig.5 *Electron temperature as a function of the position of the target with respect to the beam waist as obtained from comparison of the measurements of Fig.3 and the calculations of the code RATION shown in Fig.4.*

In the next paragraph we will see how space resolved measurements demonstrate that these average values are significantly smaller than the maximum value resulting from a spatial profile T_e.

3.2 SPATIALLY RESOLVED SPECTRA

Hereafter we will concentrate our attention to the case in which the target surface is at the beam waist. Fig.7 shows a portion of a typical space resolved spectrum obtained with the set-up of Fig.1.

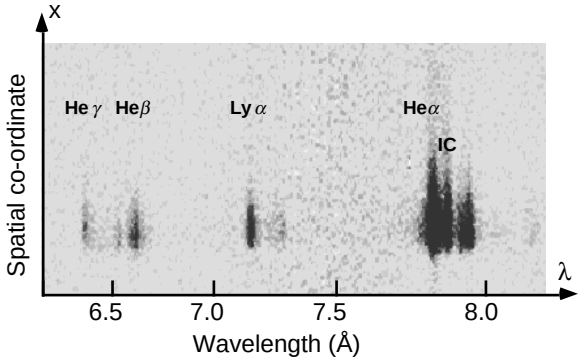

Fig.6 *Calculated Lyα to Heα intensity ratio as a function of the electron temperature and for five different electron densities.*

From this spectrum we can immediately determine the plasma longitudinal size, i.e. the size of the plasma along the normal to the target surface which is also the plasma expansion direction.

Fig shows the intensity of the Heα line as a function of the distance from the original target surface

(hereafter labelled as z). The spatial resolution is about 20 m. The size of the emitting region, defined as the FWHM of the Heα intensity profile, was found to be about 280 m.

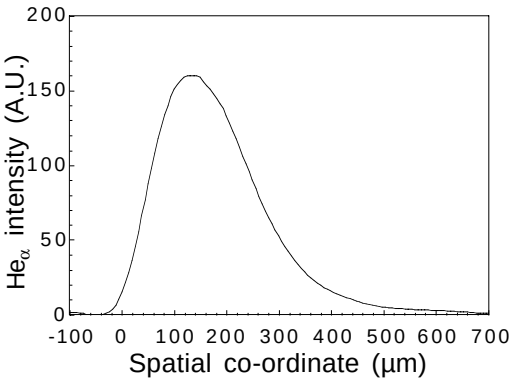

Fig.7 *Measured intensity of the Heα line emission from the plasma as a function of the distance from the target plane, This plot was obtained from the space-resolved spectrum of Fig.6 taken using the space-resolving spectrograph shown in Fig,1.*

In order to obtain a profile of electron temperature and density by comparison with RATION simulations we studied the spatial behaviour of two line intensity ratios, namely the Lyα to Heβ and the Heα to IC. Owing to the collisional coupling between $1s2p$ states of helium-like ions, this last ratio is a rapidly varying function of the electron density [12]. Fig.8 shows the spatial behaviour of the two line intensity ratios. The spatial region of investigation was limited to about 320 m since Lya and Heb line intensities decrease rapidly for larger distances.

The comparison of these ratios with RATION simulations performed for different plasma sizes yields the electron density and temperature at the boundaries of the examined region, i.e. for $z \le 75\,\mu m$ and for $z \ge 200\,\mu m$. This comparison is simplified by the negligible opacity of the plasma for the selected transitions in our experimental condition. In particular for $z \ge 200\,\mu m$ we find a nearly constant temperature of about 650 eV. The analysis of the intermediate plasma region is less straightforward due to the strong density and temperature gradients expected to take place between the critical density layer and the well-underdense coronal region. A reliable comparison with atomic physics simulations would require a detailed knowledge of the density distribution. We used the 1D Lagrangian hydrodynamics code MEDUSA [13] to calculate the expected electron density profile.

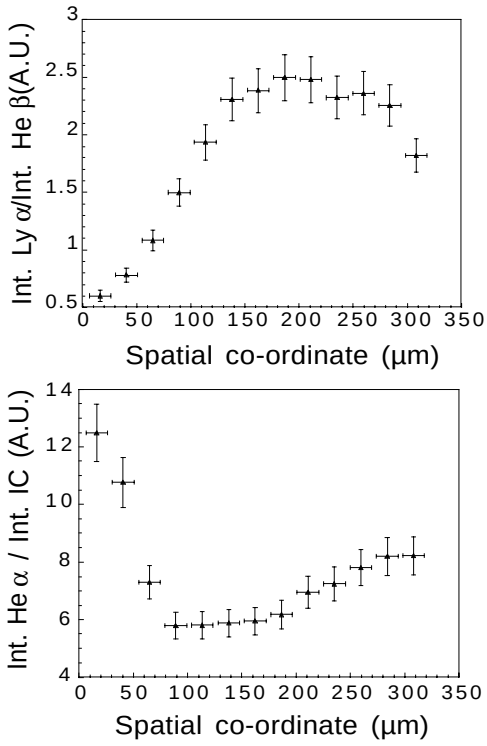

Fig.7 *Measured ratios of* Lyα to Heβ *and* Heα to IC *intensities as a function of the distance along the plasma expansion direction.*

The solid curve of Fig.9 shows the density profile calculated by MEDUSA in our interaction conditions. However, we point out here that the use of a 1D simulation to describe our interaction condition results in a serious overestimation of the electron density for distances from the target plane much greater than the plasma transverse dimension [14].

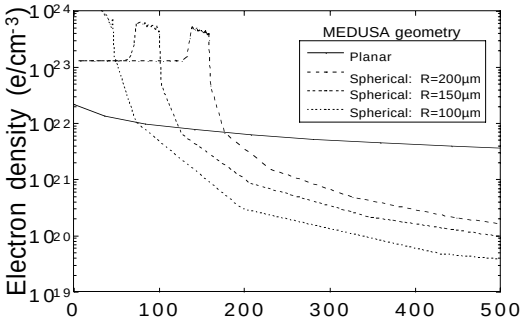

Fig.9 *Electron density profile as calculated by MEDUSA in the standard planar geometry and in the spherical geometry for three values of the radius.*

Previous studies performed by our group showed in

fact a considerable discrepancy between 1D electron density profile simulation and experimental profiles obtained by interferometric techniques [15]. As shown in Fig.9, in the experimental condition considered in this work MEDUSA simulations performed in a planar geometry give a nearly constant electron density ($\approx 10^{22}$ el/cm^3) over the whole 500 m range. This result is in clear disagreement with the results obtained for $z \leq 200\,\mu$m, where an electron density of the order of 10^{20} el/cm^3 can be inferred from comparison with RATION simulations.
We have successfully overcome this problem using an option of MEDUSA to run simulations in a 1D spherical interaction geometry, instead of the planar geometry. In fact, we found that such a geometry resulted in a more reliable prediction of electron density profiles than the planar geometry for distances from the target much greater than the initial plasma transverse dimension size. Here by initial plasma transverse size we refer to the transverse size at the beginning of the plasma formation process, i.e. to the laser focal spot diameter (¯10 m). MEDUSA was therefore set to perform hydrodynamic simulations of our experimental conditions by simulating a uniform irradiation of a spherical target. The result is shown in Fig.9 where the density profiles obtained at the peak of the pulse are shown for three different target radii. The simulation corresponding to a target radius of 100 m provided density values well in agreement with our estimation from spectroscopic measurements in the external regions (for $z \leq 75\,\mu$m and for $z \geq 200\,\mu$m).

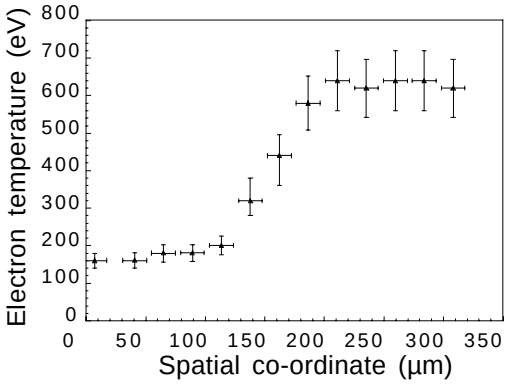

Fig.10 Electron temperature profile of the plasma produced by laser irradiation of a solid Al target by a ns Nd laser. The spatially-resolved measurement was carried out using a space-resolving X-ray crystal spectrometer equipped with a high dynamic range cooled CCD detector.

Therefore we used this electron density profile of the plasma to carry out the comparison of the Lyα to Heβ intensity ratio with RATION simulations so as to complete the electron temperature profile in the intermediate region between $z \leq 75\,\mu$m and for $z \geq 200\,\mu$m.
The final electron temperature profile is shown in Fig.10. According to this plot the electron temperature in the overdense region is slightly lower than the temperature obtained by spatially integrated spectra. In contrast, the temperature rises to much grater values in the coronal region, where the strong laser energy deposition occurs. These results clearly show that space-resolved measurements are indeed necessary in the investigation of laser-produced plasma parameters and in particular in the case of plasmas produced by laser interaction with solid targets where strong temperature/density gradients exist. Additional problems may arise from temporal integration [16] which still exists in our measurements. However, previous experiments have demonstrated that X-ray emission intensity closely follows the laser pulse intensity. Therefore we can considered the results of time integrated measurements as characteristic of the peak of the pulse, with time-smearing effects playing only a negligible effect.

4. CONCLUSIONS

The use of a space-resolving Bragg X-ray crystal spectrometer equipped with a 10 m slit coupled to a high dynamic range cooled CCD camera allowed us to obtain X-ray spectra with high spatial resolution. This high spatial resolution was only possible thanks to the use of a high sensitivity, high dynamic range cooled CCD detector.
The spectra obtained in these conditions clearly show that large electron temperature and density differences exist in our plasmas over a longitudinal extent of 320 m from the target surface. A temperature profile was obtained which shows that the electron temperature ranges from around 200 eV in the overdense region up to about 650 eV in the coronal region. These results have been compared with the results obtained from spatially integrated spectra which give an *integrated* temperature of approximately 240 eV.
Despite the small size of plasmas produced in our experimental conditions, our study clearly demonstrates the effectiveness of our space-resolved measurements in detecting large temperature and density gradients in a sub-millimetre scale plasma.

[1] D. Giulietti & L.A.Gizzi, Rivista Nuovo Cimento, **21**, n.10 (1998)
[2] R.Kauffman, in Handbook of Plasma Physics, edited by A. Rubenchik and R.Z. Sagdeev, Vol. **3** (North-Holland, Amsterdam) 1991
[3] H.R.Griem H.R., Principles of Plasma Spectroscopy, (Cambridge University Press) 1997.
[4] E. Leboucher-Dalimier, A. Poqu russe, P. Angelo, Phys. Rev. E **47**, 1467 (1993).
[5] M. Nantel, A. Klisnick, G. Jamelot P.B. Holden, B. Rus, A. Carillon, P. Jaegl , Ph. Zeitoun, G. Tallents, A.G. MacPhee, C.L.S. Lewis, S. Jacquemot, L. Bonnet, Phys. Rev. E **54**, 2852 (1996).
[6] S. Marzi, A. Giulietti, D. Giulietti, L.A. Gizzi, A. Salvetti, Laser Part. Beams, **18**, 1 (2000).
[7] A.A.Hauer, N.D. Delamater, Z.M.Koenig, Laser Part. Beams, **9**, 3 (1991).
[8] R.W. Lee, B.L. Whitten, R.E. Stout, J. Quant Spectrosc. Radiat. Transfer, **32**, 91 (1984).
[9]A. Macchi A., D. Giulietti S. Bastiani A. Giulietti, L.A. Gizzi, Nuovo Cimento D, **18**, 727 (1996).
[10]L.A. Gizzi, D. Giulietti, A. Giulietti, T. Afshar-Rad, V. Biancalana, P. Chessa, C. Danson, E. Schifano, S.M. Viana, O. Willi, Phys. Rev. E **49**, 5628 (1994).
[11] D.Giulietti, S. Bastiani, T. Ceccotti, A. Giulietti, L.A. Gizzi, A. Macchi, Nuovo Cimento D **17**, 401 (1995).
[12] D.Duston and J. Davis, Phys. Rev. A **21**, 1664 (1980).
[13] J.P.Christiansen, D.E. Ashby, K.V. Roberts, Comput. Phys. Commun. **7**, 271 (1974); P.A. Rodgers, A.M. Rogoyski, S.J. Rose}, RAL Report No. RAL-89-127, 1989 (unpublished).
[14] C.E.Max, in Laser-Plasma Interaction, Proceedings of the Ecole d' t de physique th orique, Les Houches, session XXXIV}, edited by Balian R. and Adam J.-C. (North-Holland, Amsterdam) 1982.
[15] L.A. Gizzi, D. Giulietti, A. Giulietti, T. Afshar-Rad, V. Biancalana, P. Chessa, C. Danson, E. Schifano, S.M. Viana, O. Willi, Phys. Rev. E **49**, 5628 (1994).
[16] D. Duston, R.W. Clark, J. Davis, J.P. Apruzese, Phys. Rev. A **27**, 1441 (1983).